IEEE Access
Multidisciplinary | Rapid Review | Open Access Journal

Received July 7, 2018, accepted August 17, 2018, date of publication August 29, 2018, date of current version October 12, 2018.

Digital Object Identifier 10.1109/ACCESS.2018.2867624

A Short-Circuit Calculation Method for DFIG-Based Wind Farms

MINGYANG LIU[1], WENXIA PAN[1,2], RUI QUAN[1], HONGYU LI[1], (Student Member, IEEE), TONGCHUI LIU[1,3], AND GANG YANG[4]

[1]College of Energy and Electrical Engineering, Hohai University, Nanjing 210098, China
[2]Research Center for Renewable Energy Generation Engineering of Ministry of Education, Hohai University, Nanjing 210098, China
[3]State Grid Ningbo Power Supply Company, Ningbo 315200, China
[4]Maintenance Branch of Jiangsu Electric Power Company, Xuzhou 221000, China

Corresponding author: Wenxia Pan (pwxhh@hhu.edu.cn)

This work was supported in part by the National Natural Science Foundation of China under Grant 51377047, in part by the "111" project of "Renewable Energy and Smart Grid" under Grant B14022, in part by the Postgraduate Research & Practice Innovation Program of Jiangsu Province under Grant KYCX18_0544, and in part by the Fundamental Research Funds for the Central Universities of China under Grant 2018B674X14.

ABSTRACT Short-circuit calculations for wind farms are crucial for determining equipment ratings and providing basic information for protection coordination. In this paper, a practical calculation method of short-circuit currents (SCCs) is proposed for doubly fed induction generator (DFIG)-based wind farms. The improved calculation method of the SCCs in single DFIG is developed based on electromagnetic transient analysis. Combined with the traditional method of calculating the SCCs of the power system, an equivalent model of the DFIG-based wind farm used for SCCs is studied. The equivalent model and expressions for SCCs are later validated through PSCAD/EMTDC-based simulation results, and a comparison with the national standard calculation method is analyzed. The results show that the calculation method proposed in this paper has better accuracy and practicability, which are important elements in the electrical design of DFIG-based wind farms.

INDEX TERMS Wind farm, doubly-fed induction generator (DFIG), short-circuit current, symmetrical fault.

I. INTRODUCTION

Wind, as a clean and economically feasible source of electrical energy, has recently been gaining special attention [1], [2]. In China, a large number of doubly-fed induction generators (DFIGs) connect to the grid in the form of clusters, resulting in a threat to the safe and stable operation of the grid [3], [4]. Short-circuit current calculation methods for power systems with wind turbines are very important because they are the key to analyzing the influence of wind turbine access to grids and developing new protection principles. Usually, chopper and crowbar protection are used in DFIGs to improve their capabilities for low voltage ride through (LVRT) [5], [6], but the fault characteristics of DFIGs with the crowbar protection are hence changed [7], and the topology becomes more complex especially when crowbar protection in several DFIGs are activated simultaneously [8]. Even though the power system with a DFIG-based wind farm is complicated, it is still necessary to study an accurate and simplified calculation method for SCCs.

In previous studies, some transient fault models and calculation methods for DFIGs have been reported, such as [9]–[11]. However, works on single wind turbine systems are currently insufficient for describing the characteristics of large numbers of units, especially taking into account increasing wind power integration capacity. A novel modeling technique for a Type 3 wind farm based on the generalized averaging theory is proposed in [12]. A comprehensive modeling and stability analysis framework of a weak grid that interfaces an LCC-HVDC station and a DFIG-based wind farm is developed in [13]. An impedance protection circuit configuration to enhance the ride-through of DFIGs based wind turbines during faults is proposed in [14]. A method for calculating the SCC of DFIG-based wind farms considering the influence of inverter control is provided in [15]. And based on the improved LVRT control, the nonlinear dynamic model of wind farms under symmetric and asymmetric faults is studied in [16]. In addition, based on the analysis of DFIGs' transient characteristics, the equivalent model of doubly-fed wind plants is discussed in [17] and [18]. However, most of the methods need many parameters and the calculation process is relatively complex, so that these methods cannot be applied to the practical calculation directly. Therefore, the studies on the SCCs calculation for DFIG-based wind farms for engineering applications are beginning to receive

attention from researchers. Compared with [19], this paper has a new approach. The relationship between theoretical parameters and easy-to-obtain parameters is analyzed in detail, and the calculation method of SCC instantaneous value under theoretical analysis and improved algorithm is given. Moreover, the practical calculation formula of SCC in wind farms is given.

The main scope of this study is to find a SCCs calculation method for DFIG-based wind farms, which could be applied to engineering practice well. Thus, in this paper, based on the EMT analysis, the influence of crowbar on SCCs of DFIG is firstly analyzed. Then an improved method suitable for an engineering application is proposed according to the relationship between unknown parameters and ready-to-use parameters. Moreover, considering transfer impedance of collector lines, the equivalent impedance model of DFIGs under different connection types is established and a calculation method for SCCs in DFIG-based wind farms is also carried out. Finally, the accuracy of the proposed practical method is verified by the comparison with the simulation results from PSCAD/EMTDC (Power Systems Computer Aided Design/ Electromagnetic Transients including DC). In addition, a comparison between the proposed practical method and the national standard [20] calculation method in China is analyzed in this paper.

II. ANALYSIS OF SCCS FOR DFIG CONSIDERING CROWBAR PROTECTION

There are some differences between general induction generators (IGs) and DFIGs with crowbar protection. For the power system with DFIGs, the SCC calculation method for IGs may not work well. In this section, based on the EMT analysis of DFIGs with crowbar protection, a SCC calculation method for DFIGs is analyzed, which is called theoretical analysis.

Figure 1 shows a simple doubly-fed wind turbine system. The DFIG has been interconnected with the grid in which the stator of the generator is directly connected with the grid whereas, the rotor get connected through a Back-to-Back converter arrangement as shown in Figure 1. The converters are known as the rotor side converter (RSC) and the grid side converter (GSC) and these two are connected cascaded through a DC-link capacitor placed between them. The GSC controls the DC-link voltage independent of the rotor power and the RSC controls the rotor currents [6]. During severe fault conditions, in order to ensure the safety of the DFIG, the crowbar protection will be activated to short circuit the rotor windings and divert the surge current from the rotor-side converter (RSC) [10].

In this paper, the transient process is mainly considered to be caused by the instant symmetrical short-circuit fault, which usually brings the most serious impacts to the power grid than other faults. It is considered that the overall DFIG system is at a stage where the control system is not in operation, or is working, but has not reached a steady state. Also, the wind speed and the speed of the generator are assumed to be the same as pre-fault [21]. The EMT equations of DFIG in

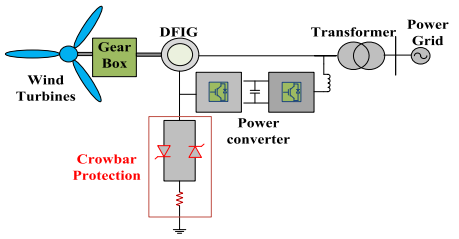

FIGURE 1. Diagram of simple doubly-fed wind turbine system.

a synchronously rotating reference frame are given by

$$\boldsymbol{u}_s = R_s\boldsymbol{i}_s + \mathrm{j}\omega_s\psi_s + \mathrm{d}\boldsymbol{\psi}_s/\mathrm{d}t \quad (1)$$

$$\boldsymbol{u}_r = R_r\boldsymbol{i}_r + \mathrm{j}\omega_p\boldsymbol{\psi}_r + \mathrm{d}\boldsymbol{\psi}_r/\mathrm{d}t \quad (2)$$

$$\boldsymbol{\psi}_s = L_s\boldsymbol{i}_s + L_m\boldsymbol{i}_r \quad (3)$$

$$\boldsymbol{\psi}_r = L_m\boldsymbol{i}_s + L_r\boldsymbol{i}_r \quad (4)$$

where $\boldsymbol{u}, \boldsymbol{i}, R, L, \boldsymbol{\psi}$ are the voltage and current, resistance, inductance, and flux, respectively; and the subscripts s and r represent the stator winding and rotor winding, respectively. $L_s = L_{s\sigma} - L_m$ and $L_r = L_{r\sigma} - L_m$, where $L_{s\sigma}$ and $L_{r\sigma}$ are the stator leakage inductance and rotor leakage inductance, respectively. L_m is the magnetizing inductance, ω_p is the slip angular velocity, and ω_s is the synchronous speed.

Then, according to Equations (3) and (4), the SCC of stator and rotor can be expressed as

$$\boldsymbol{i}_s = -k_r\boldsymbol{\psi}_r/L'_s + \boldsymbol{\psi}_s/L'_s \quad (5)$$

$$\boldsymbol{i}_r = -k_s\boldsymbol{\psi}_s/L'_r + \boldsymbol{\psi}_r/L'_r \quad (6)$$

where L'_s and L'_r represent the transient inductance of stator winding and rotor winding, respectively. $L'_\mathrm{s} = L_{s\sigma} + L_{r\sigma}L_\mathrm{m}/(L_{r\sigma} + L_\mathrm{m})$, and $L'_\mathrm{r} = L_{r\sigma} + L_{s\sigma}L_\mathrm{m}/(L_{s\sigma} + L_\mathrm{m})$. k_s and k_r denote the inductance coupling coefficient of stator and rotor, respectively. $k_\mathrm{s} = L_\mathrm{m}/L_\mathrm{s}$, and $k_\mathrm{r} = L_\mathrm{m}/L_\mathrm{r}$.

When a serious symmetrical fault occurs, in order to avoid converter being damaged by a too-large rotor current, the RSC is quickly locked by the control system, and crowbar resistance is connected [22], [23]. During symmetrical faults, the maximum value of SCC usually appears in the process between the crowbar insertion and RSC re-starting [3], so the SCC calculation in this paper is mainly analyzed based on this process. Meanwhile, in this process, the power electronic control system has seldom effects on the maximum values of SCC because the RSC is quickly locked. Therefore, the influence of control system is not considered in this paper.

To make the analysis easily, we assume the symmetrical short circuit occurs at $t = t_0$, and the crowbar is inserted at $t = t_0^+$. Then, a transient equivalent circuit can be established, which is shown in Figure 2.

According to the stator equivalent impedance presented in [24] and using the Thevenin's theorem, the equivalent impedance of the stator side considering crowbar protection can be deduced as Equation (7).

$$Z_\mathrm{s} \approx \mathrm{j}\omega_\mathrm{s}L_{s\sigma} + [(R_\mathrm{CB} + \mathrm{j}\omega_\mathrm{s}L_{r\sigma})//j\omega_\mathrm{s}L_\mathrm{m}] = R_\mathrm{CB} + \mathrm{j}\omega_\mathrm{s}L'_\mathrm{s} \quad (7)$$

where R_CB is the crowbar resistance.

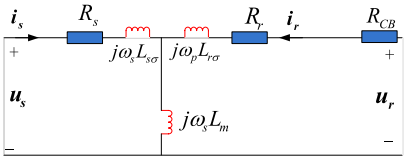

FIGURE 2. The equivalent circuit of a DFIG with the element of crowbar resistance for transient analysis.

Assuming the stator voltage falls to U_{s1}, the voltage drop factor of stator side is defined as per Equation (8)

$$K_d = (U_{s0} - U_{s1})/U_{s0} \tag{8}$$

where U_{s0} is the voltage of stator side before symmetrical short-circuit occurs.

According to the magnetic flux linkage conservation law and the EMT Equations (1), (2), (7), and (8), the expression of the magnetic chain at the stator side and rotor side after the fault can be derivate, which are as shown in Equations (9) and (10):

$$\psi_s = (1 - K_d)U_{s0}e^{j\omega_s t}/(j\omega_s) + K_d U_{s0}e^{-t/\tau_s}/(j\omega_s) \tag{9}$$

$$\psi_r = L_r(U_{s0} - Z_s I_{s0})e^{j\omega_s t}e^{-t/\tau_r}/(j\omega_s L_m) \tag{10}$$

where I_{s0} is the current of stator side before symmetrical short-circuit occurs, τ_s and τ_r represent the transient time constant of stator and rotor, respectively. $\tau_s = L'_s/R_s$, and $\tau_r = L'_r/R_r$.

Inserting Equations (9) and (10) into Equation (5), based on the coordinate system transformation method, the expression of the A-phase SCC of a DFIG in a fixed reference frame can be estimated by Equation (11).

$$\begin{aligned} i_{sa} = {} & \frac{(1 - K_d)U_{s0}}{\omega_s L'_s}\cos(\omega_s t + \alpha) + \frac{K_d U_{s0}}{\omega_s L'_s}e^{-\frac{t}{\tau_s}}\cos\alpha \\ & - \frac{1}{\omega_s L'_s}[U_{s0} - (R_{CB} + j\omega_s L'_s)I_{s0}]\cos(\omega_s t + \alpha)e^{-\frac{t}{\tau'_r}} \end{aligned} \tag{11}$$

where α is the voltage initial phase angle.

According to the description of the maximum short circuit current in [4], when $\alpha = 0$ and $t = T/2$, the effective value of Equation (11) (i.e., the effective value of periodic component of SCC) is expressed as

$$I_G \approx \frac{U_{s0} - \sqrt{\omega_s^2 L_s'^2 + R_{CB}^2}I_{s0}}{\sqrt{2}\omega_s L'_s} - \frac{(1 - K_d)U_{s0}}{\sqrt{2}\omega_s L'_s} \tag{12}$$

Due to several unknown parameters (e.g., ω_s, L'_s, R_{CB}, U_{s0}, and I_{s0}), Equation (12) cannot be applied to the practical calculation directly. Meanwhile, in Chinese standard GB/T15544.1 (''three-phase AC system SCC calculation'', see [20]), an engineering calculation method for SCC is proposed based on the ready-to-use from the generator manufacturer, but its accuracy is not satisfied. Hence, in the following Section, an improved calculation method is proposed based on Equation (12) for SCCs, by using the ready-to-use parameters which are adopted in the Chinese national standard GB/T15544.1. In other words, the proposed practical method takes advantage of method based on Equation (12) and the method offered by the Chinese national standard GB/T15544.1.

III. AN IMPROVED CALCULATION METHOD FOR SCCS OF DFIGS CONSIDERING CROWBAR PROTECTION

To offer the improved method with high accuracy and only using ready-to-use parameters, it is necessary to get the relationship between the unknown and ready-to-use parameters. In this Section, based on the locked rotor test principle and the DC test principle [25], the unknown parameters in Equation (12) are expressed by the ready-to-use parameters provided by generator manufacturers.

In the case of blocking, the excitation branch in the equivalent circuit of a DFIG can be ignored, because $|R_r + j\omega_s L_{r\sigma}| \ll |j\omega_s L_m|$ [25]. Furthermore, the input impedance of each phase can be expressed as follows [25]:

$$Z_{br} = R_s + R_r + j\omega_s(L_{s\sigma} + L_{r\sigma}) = R_{eq} + j\omega_s L_{eq} \tag{13}$$

where $R_{eq} = R_s + R_r$ and $L_{eq} = L_{s\sigma} + L_{r\sigma}$.

According to the locked rotor test principle in [25], R_{eq}, Z_{br}, and $\omega_s L_{eq}$ are as follows:

$$R_{eq} = P_{br}/I_{br}^2 \tag{14}$$

$$Z_{br} = U_{br}/I_{br} \tag{15}$$

$$\omega_s L_{eq} = (Z_{br}^2 - R_{eq}^2)^{1/2} \tag{16}$$

where P_{br} is the input power of the single phase. U_{br} is the input phase voltage, and I_{br} is the input current.

For DFIGs with the megawatt capacity, the values of R_s and R_r are far lower than those of $j\omega_s L_{s\sigma}$ and $j\omega_s L_{r\sigma}$, and have seldom impact on the calculations. Thus, R_s and R_r can be estimated by Equation (17)

$$R_s = R_r = R_{eq}/2 = P_{br}/(2I_{br}^2) = P_{rM}/(6I_{LR}^2) \tag{17}$$

where P_{rM} is the motor-rated power, and $P_{rM} = 3P_{br}$. I_{LR} is the locked-rotor current, and $I_{LR} = I_{br}$.

According to the test and analysis of large and medium asynchronous motor in [26], $\omega_s L_{s\sigma}$ and $\omega_s L_{r\sigma}$ can be deduced as

$$\omega_s L_{s\sigma} \approx \omega_s L_{r\sigma} \approx \omega_s L_{eq}/2 = (3U_{rM}^2 I_{LR}^2 - P_{rM}^2)^{1/2}/6I_{LR}^2 \tag{18}$$

where U_{rM} is the motor-rated voltage, and $U_{rM} = \sqrt{3}\,U_{br}$.

Furthermore, due to $L_{r\sigma} \ll L_m$, the L'_s and L'_r can be estimated using Equation (19)

$$L'_s \approx L_{s\sigma} + L_{r\sigma} \approx L'_r. \tag{19}$$

Incorporating Equations (18) and (19) into Equations (11) and (12), the new value expressions of SCC are shown as

follows

$$i_{sa} \approx \frac{3I_{LR}^2(1-K_d)U_{rM}}{\sqrt{3U_{rM}^2I_{LR}^2-P_{rM}^2}}\cos(\omega_s t+\alpha) + \frac{3I_{LR}^2K_dU_{rM}}{\sqrt{3U_{rM}^2I_{LR}^2-P_{rM}^2}}e^{-\frac{t}{\tau_S}}\cos\alpha - \frac{3I_{LR}^2}{\sqrt{3U_{rM}^2I_{LR}^2-P_{rM}^2}} \times [U_{rM}-(R_{CB}+j\frac{\sqrt{3U_{rM}^2I_{LR}^2-P_{rM}^2}}{3I_{LR}^2})I_{rM}] \times \cos(\omega_s t+\alpha)e^{-\frac{t}{\tau_r}} \quad (20)$$

$$I_G = \frac{3U_{rM}I_{LR}^2-\sqrt{3U_{rM}^2I_{LR}^2-P_{rM}^2+9I_{LR}^4R_{CB}^2}I_{rM}}{\sqrt{6U_{rM}^2I_{LR}^2-2P_{rM}^2}} - \frac{3I_{LR}^2(1-K_d)U_{rM}}{\sqrt{6U_{rM}^2I_{LR}^2-2P_{rM}^2}} \quad (21)$$

where U_{rM}, I_{rM}, I_{LR}, and P_{rM} are easy to be obtained from the generator manufacturers. The crowbar resistance RCB may not be offered by the manufacturer, but is also can be calculated by a scheme in [27].

The SCC curves calculated by the three ways (i.e., simulation, theoretical analysis and improved method) are shown in Figure 3. The red curve in Figure 3 is the PSCAD-based simulation results. The blue curve in Figure 3 is calculated by Equation (11), corresponds to theoretical analysis. The black curve in Figure 3 is calculated by Equation (20), corresponds to improved method. The comparisons the SCC maximum value and its appearance time in the three methods are shown in Tables 1 and 2, respectively. In the comparisons, the relative error $e\%$ is adopted to describe the accuracy of the method, and $e\% = (I_{Equation} - I_{simulation})/ \times 100\%$, where $I_{Equation}$ denotes the SCC results from the methods (i.e., theoretical analysis and improved method) to be studied and $I_{simulation}$ denotes the SCC results from the simulation in PSCAD/EMTDC.

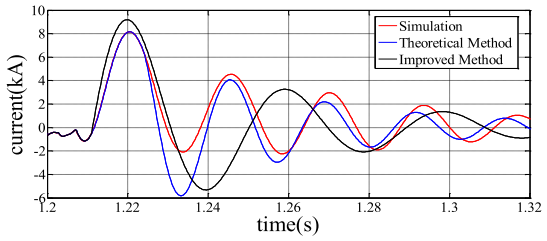

FIGURE 3. The simulation result of the short circuit current.

At the same time, the accuracy of the Equations (12) and (21) is verified by comparing the simulation results of PSCAD/EMTDC, which are as shown in Table 3.

The results in Tables 1, 2 and 3 show that the calculated error between simulation and theoretical method is small, which ensure the accuracy of calculation method. And the calculated error between simulation and improved method is bigger but is acceptable. Thus, the effectiveness and feasibility of the theoretical method and improved method are verified.

TABLE 1. Time comparison of the maximum of the SCC.

	t_{Imax}/s	e%
Simulation value	1.22050	-
Theoretical analysis	1.22075	0.02%
Improved method	1.21975	-0.061%

TABLE 2. Comparison of the maximum value of the SCC.

	Imax/kA	e%
Simulation value	8.158	-
Theoretical analysis	8.162	0.049%
Improved method	9.188	12.6%

TABLE 3. The Results of the SCC.

	SCC/kA	e%
Simulation value	2.604	-
Theoretical analysis	2.646	1.61%
Improved method	2.732	4.92%

IV. PRACTICAL CALCULATION METHOD FOR SCCS IN DFIG-BASED WIND FARMS

As the DFIG-based wind farms usually consists of multiple small capacity units, when a symmetrical fault occurs at the point of common coupling (PCC), the calculation efficiency will be affected when estimating the SCC contributed by each DFIG. Therefore, the cluster may be equivalent to a voltage source for research [28].

In Figure 4, a simple DFIG-based wind farm is shown. In this paper, the number of the DFIGs cluster is defined as n, in which two kinds of connection way for the cluster are considered. Meanwhile, they are grouped according to the connection type categories. In the system, the groups from

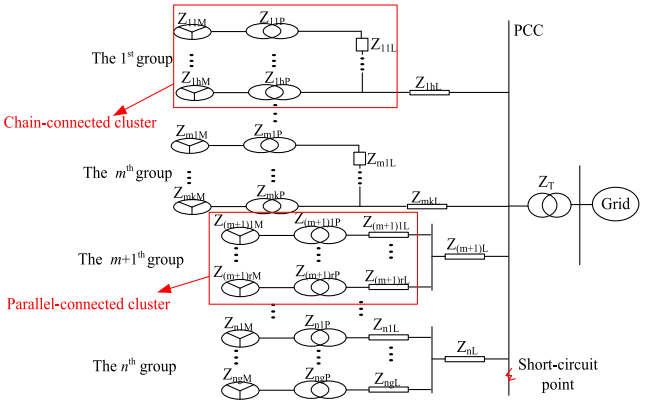

FIGURE 4. Main wiring diagram of the system.

the first group to m^{th} group are chain-connected clusters, and the groups from $m+1^{\text{th}}$ group to n^{th} group are parallel-connected clusters.

According to the definition of the initial symmetrical SCC (i.e., the effective value of a periodic component of the SCC) and the peak short-circuit current (PSCC) [20], the expression are as follows

$$I''_{\text{k}} = I''_{\text{k}*} \cdot S_{\text{d}}/(\sqrt{3}\, U_{\text{d}}) = (1/Z_{\text{k}*}) \cdot S_{\text{d}}/(\sqrt{3}\, U_{\text{d}}) \quad (22)$$

$$i_{\text{sh}} = \sqrt{2} I''_{\text{k}} \cdot (1 + \text{e}^{-0.01/T_{\text{a}}}) \quad (23)$$

where U_{d} and S_{d} are reference voltage and reference capacity, respectively. $I''_{\text{k}*}$ is the per-unit value of SCC. $Z_{\text{k}*}$ is the short-circuit total impedance (p.u.). T_{a} is the attenuation time constant of the DC component of SCC, $T_a = X_\Sigma/\omega R_\Sigma$, X_Σ and R_Σ are the short-circuit reactance and short-circuit resistance, respectively, from the point of the fault to the power source.

Introducing $I''_{\text{k}} = I_{\text{G}}$ into Equation (22), the equivalent impedance of DFIG can be estimated as follows:

$$Z_{M*} = \frac{\sqrt{6U_{rM}^2 I_{LR}^2 - 2P_{rM}^2}}{3K_d U_{rM} I_{LR}^2 - \sqrt{3U_{rM}^2 I_{LR}^2 - P_{rM}^2 + 9I_{LR}^4 R_{CB}^2 I_{rM}}} \cdot \frac{S_{\text{d}}}{\sqrt{3}\, U_{\text{d}}} \quad (24)$$

where Z_{M*} is the per-unit value of the impedance of DFIG, and the subscript $*$ represents the per-unit value.

The equivalent impedance of other elements in the DFIG-based wind farm can also be calculated using the traditional method in [29]. In the traditional practical calculation method for SCC, the principle of the series and parallel circuit is usually used to simplify the grid topology. However, as the particularity of the chain-connection of the DFIGs is different from the ordinary synchronous generator, with the method of the single weighted and equivalent power loss [30], a simplified equivalent model is completed, which is as shown in Figure 5. The short-circuit impedance calculated by the proposed practical method is larger than that obtained by traditional series and the parallel method (a detailed analysis can be found in Appendix B).

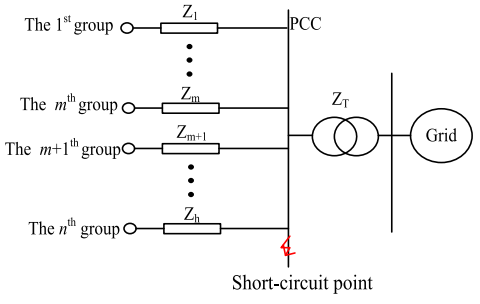

FIGURE 5. Diagram of the system after independent group equivalence.

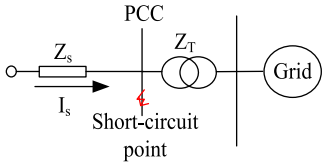

FIGURE 6. The diagram of the system after all groups equivalents.

In the chain cluster (i.e., $i = 1 \sim m$), the expression of the equivalent impedance is as follows:

$$Z_{i*} = \left[\sum_{j=1}^{nP} n_{ij}^2 \left(Z_{ijM*} + Z_{ijP*} \right) + \sum_{j=1}^{nP} \left(\sum_{k'=1}^{j} n_{ik'} \right)^2 Z_{ijL*} \right] / \left(\sum_{j=1}^{nP} n_{ij} \right)^2 \quad (25)$$

In the parallel cluster (i.e., $i = m+1 \sim n$), the expression of the equivalent impedance is given as follows:

$$Z_{i*} = \left(\sum_{j=1}^{nP} n_{ij}^2 \left(Z_{ijM*} + Z_{ijP*} + Z_{ijL*} \right) \right) / \left(\sum_{j=1}^{nP} n_{ij} \right)^2 + Z_{iL*} \quad (26)$$

where Z_{i*} is the per-unit value of the impedance of i^{th} DFIG, which is also as shown in Figure 4. The subscript i represents the serial number of a group. nP is the number of DFIGs in the i^{th} group. Z_{ijP*} is the impedance of transformer. Z_{ijL*} is the line impedance. n_{ij} ($n_{ik'}$) represents the ratio of the DFIG rated current to the DFIG reference current of the j^{th} (k'^{th}) DFIG in the i^{th} chain; Z_{iL*} is the line impedance between the bus bar of the i^{th} group and the PCC.

As shown in Figure 5, the equivalent connection is similar to the parallel connection, so the expression of the equivalent short-circuit impedance of the whole DFIG clusters system can be reduced as:

$$Z_{k*} = Z_{S*} = \left(\sum_{i=1}^{n} n_i^2 Z_{i*} \right) / \left(\sum_{i=1}^{n} n_i \right)^2 \quad (27)$$

where Z_{S*} is the short circuit total impedance (p.u.), and n_i is the ratio of the rated current to reference current of the cluster in the i^{th} group.

The equivalent circuit of DFIG-based wind farm is as shown in Figure 6.

Finally, based on Equations (22), (23) and (27), the SCC and the PSCC of the DFIG-based wind farm can be estimated, which provide the critical information for selecting the appropriate electrical equipment.

V. SIMULATION AND RESULT ANALYSIS

A simple network as Figure 7 shown is built in PSCAD/EMTDC which is the commercial math software produced by the 211 Commerce Drive company in Winnipeg,

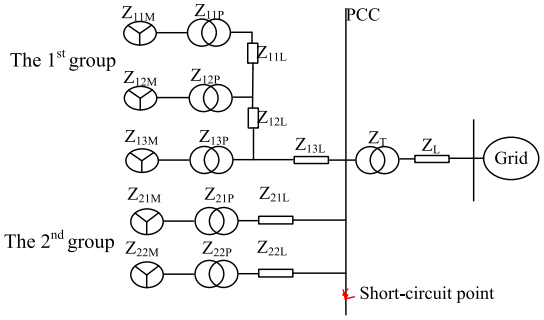

FIGURE 7. Diagram of the simulation system.

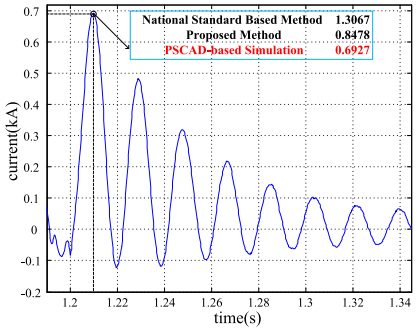

FIGURE 8. The simulation result of the short-circuit current.

TABLE 4. Results of the short-circuit current calculation.

	SCC/kA	PSCC/kA
PSCAD-based simulation	0.4607	0.6927
Proposed practical method	0.4996	0.8478
National standard based method	0.5327	1.3067

Manitoba, Canada to verify the proposed short-circuit currents calculation method for the DFIG-based wind farms. It is characterized by the detailed data and high reliability of the simulation results. Therefore, the error of simulation results is not discussed in this paper. In order to simulate fault currents under a fault, the wind speed is set as 8 m/s, the grid equivalent impedance is 1.2 p.u., and the symmetrical short-circuit at PCC (35 kV) occurs at 1.2 s. The DFIG parameters are given in Appendix A.

In this case, the SCCs are calculated by using the national standard based method in [24], the proposed practical method and the PSCAD-based simulation, respectively. The SCCs from a DFIG-based wind farm are as shown in Figure 8. Three peak values calculated by three methods are 0.6927kA, 0.8478kA and 1.3067kA, respectively. It can be seen that results from the proposed practical method is closer to those from the simulation method in PSCAD which are regarded as the true values. Meanwhile, in the same case of a symmetrical short-circuit fault, the SCCs contributed by DFIG-based wind farm are calculated using three methods to further verify the accuracy of the proposed practical method, which are as shown in Table 4.

After analyzing the results of the calculations in Table 4, three points are given as follows:

a) Compared with the simulation results of SCC, the error of the practical SCC calculation method proposed in this paper is only 8.4%, which means the accuracy of the proposed practical method is high. Meanwhile, compared with the error of the national standard method (i.e., 15.6%), the method proposed in this paper significantly improves the calculation accuracy.
b) Compared with the error of the national standard method (i.e., 88.64%), the error of the short-circuit impulse current calculated by this method is about 22.39%. In other words, the error caused by the proposed practical method represents only about one-quarter of the error in the national standard based method. Therefore, the computational accuracy of the proposed practical method is better than that of the national standard based method.
c) Both the proposed practical method and the national standard based method resulted in values larger than those obtained in the simulation results. This is because the process is simplified in terms of computational efficiency and some errors are brought in the engineering calculation method. Even though the results from the proposed practical method are bigger than the true values, it does not a bad thing. Security is the most important characteristic of the power system. If the results of engineering method will be larger than the simulation results, the corresponding selected electrical equipment is safer.

VI. CONCLUSIONS

In this paper, an improved SCC calculation method for DFIG-based wind farms is proposed. Firstly, a SCC calculation method of a single DFIG is analyzed by studying the DFIG electromagnetic transient process. Secondly, an improved SCC calculation method which can be applied to engineering practice is proposed by studying the relationship between unknown and ready-to-use parameters in the nameplate. Thirdly, with the influence of the complex cluster topology and the different connection types of DFIGs, a practical SCC calculation method of the DFIG-based wind farm is proposed. Finally, a validation study is performed using a simple network with a detailed PSCAD-based simulation model for the DFIGs. The simulation results confirm the accuracy and practicability of the presented method.

Due to its practicability and higher accuracy, the presented method provides the more reliable information for selecting appropriate electrical equipment. Also, this paper provides a new method and insight for improving the engineering standards for short circuit current calculation of DFIG-based wind farms.

APPENDIX

A. DFIG PARAMETERS

$U_{rM} = 0.69$ kV, $P_{rM} = 1$ MW, $L_{s\sigma} = 0.1$ pu, $L_{r\sigma} = 0.11$ pu, $L_m = 4.5$ pu, $R_s = 0.0054$ pu, $R_r = 0.006$ pu, $R_{CB} = 0.03$ pu, $I_{LR}/I_{rM} = 6.14$, $\cos\varphi = 0.85$.

B. A DETAILED ANALYSIS

The following simple chain structure is illustrated as an example

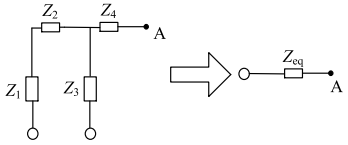

The result of the traditional practical calculation method is as follows:

$$Z_{eq(a)} = (Z_1 + Z_2)//Z_3 + Z_4 = \frac{Z_3(Z_1 + Z_2)}{Z_1 + Z_2 + Z_3} + Z_4$$

The results of the method in this paper are:

$$Z_{eq(b)} = \frac{(Z_1 + Z_3) + (Z_2 + 2^2 \cdot Z_4)}{(1+1)^2} = \frac{Z_1 + Z_3 + Z_2 + 4Z_4}{4}$$

and,

$$\begin{aligned} &Z_{eq(b)} - Z_{eq(a)} \\ &= \frac{Z_1 + Z_3 + Z_2 + 4Z_4}{4} - \frac{Z_3(Z_1 + Z_2)}{Z_1 + Z_2 + Z_3} - Z_4 \\ &= \frac{(Z_1 + Z_3 - Z_2)^2}{4(Z_1 + Z_3 + Z_2)} > 0 \\ &\Rightarrow Z_{eq(b)} > Z_{eq(a)} \end{aligned}$$

Therefore, the short circuit impedance calculated by this method is larger than that obtained using the traditional calculation method. Using Equation (21), we can see that the short circuit current calculated in this paper is smaller than that found with the traditional calculation method, and is closer to the actual value.

ACKNOWLEDGMENT

I would like to thank my respectable teacher Prof. Pan Wenxia for her time and guidance. Also, I would like to thank the other co-authors for their contribution in this work.

REFERENCES

[1] Y. Feng *et al.*, "Overview of wind power generation in China: Status and development," *Renew. Sustain. Energy Rev.*, vol. 50, pp. 847–858, Oct. 2015.

[2] S. Sun, F. Liu, S. Xue, M. Zeng, and F. Zeng, "Review on wind power development in China: Current situation and improvement strategies to realize future development," *Renew. Sustain. Energy Rev.*, vol. 45, pp. 589–599, May 2015.

[3] F. Sulla, J. Svensson, and O. Samuelsson, "Symmetrical and unsymmetrical short-circuit current of squirrel-cage and doubly-fed induction generators," *Electr. Power Syst. Res.*, vol. 81, pp. 1610–1618, Jul. 2011.

[4] P. Ju, H. Li, C. Gan, Y. Liu, Y. Yu, and Y. Liu, "Analytical assessment for transient stability under stochastic continuous disturbances," *IEEE Trans. Power Syst.*, vol. 33, no. 4, pp. 2004–2014, Mar. 2018.

[5] J. Morren and S. W. H. D. Haan, "Short-circuit current of wind turbines with doubly fed induction generator," *IEEE Trans. Energy Convers.*, vol. 22, no. 1, pp. 174–180, Mar. 2007.

[6] R. A. J. Amalorpavaraj, P. Kaliannan, S. Padmanaban, U. Subramaniam, and V. K. Ramachandaramurthy, "Improved fault ride through capability in DFIG based wind turbines using dynamic voltage restorer with combined feed-forward and feed-back control," *IEEE Access*, vol. 5, pp. 20494–20503, 2017.

[7] S. Swain and P. K. Ray, "Short circuit fault analysis in a grid connected DFIG based wind energy system with active crowbar protection circuit for ridethrough capability and power quality improvement," *Int. J. Elect. Power Energy Syst.*, vol. 84, pp. 64–75, Jan. 2017.

[8] C. Wessels, F. Gebhardt, and F. W. Fuchs, "Fault ride-through of a DFIG wind turbine using a dynamic voltage restorer during symmetrical and asymmetrical grid faults," *IEEE Trans. Power Electron.*, vol. 26, no. 3, pp. 807–815, Mar. 2011.

[9] J. Ouyang and X. Xiong, "Research on short-circuit current of doubly fed induction generator under non-deep voltage drop," *Electr. Power Syst. Res.*, vol. 107, pp. 66–158, Feb. 2014.

[10] F. Xiao, Z. Zhang, and X. Yin, "Fault current characteristics of the DFIG under asymmetrical fault conditions," *Energies*, vol. 8, pp. 10971–10992, Oct. 2015.

[11] T. Kauffmann, U. Karaagac, I. Kocar, S. Jensen, J. Mahseredjian, and E. Farantatos, "An accurate type III wind turbine generator short circuit model for protection applications," *IEEE Trans. Power Del.*, vol. 32, no. 6, pp. 2370–2379, Dec. 2017.

[12] S. Chandrasekar and R. Gokaraju, "Dynamic phasor modeling of type 3 DFIG wind generators (including SSCI phenomenon) for short-circuit calculations," *IEEE Trans. Power Del.*, vol. 30, no. 2, pp. 887–897, Apr. 2015.

[13] A. Yogarathinam, J. Kaur, and N. R. Chaudhuri, "Impact of inertia and effective short circuit ratio on control of frequency in weak grids interfacing LCC-HVDC and DFIG-based wind farms," *IEEE Trans. Power Del.*, vol. 32, no. 4, pp. 2040–2051, Aug. 2017.

[14] J. J. Justo and R. C. Bansal, "Parallel *R-L* configuration crowbar with series *R-L* circuit protection for LVRT strategy of DFIG under transient-state," *Electr. Power Syst. Res.*, vol. 154, pp. 299–310, Jan. 2018.

[15] J. Yin, Y. B. Li, J. H. Xiong, and Z. K. Yan, "Short circuit current calculation and fault analysis method of DFIG wind-farm groups," *Electr. Power Automat. Equip.*, vol. 37, no. 8, pp. 113–122, Aug. 2017.

[16] M. K. Döşoğlu, "Nonlinear dynamic modeling for fault ride-through capability of DFIG-based wind farm," *Nonlinear Dyn.*, vol. 89, no. 4, pp. 2683–2694, Sep. 2017.

[17] O. Jinxin, D. Yanbo, Z. Di, Y. Rui, Z. Xi, and X. Xiaofu, "Dynamic equivalent model of doubly fed wind farm during electromagnetic transient process," *IET Renew Power Gen.*, vol. 11, pp. 100–106, Jan. 2017.

[18] Y. H. Yan and W. Feng, "Short-circuit current analysis for DFIG wind farm considering the action of a crowbar," *Energies*, vol. 11, no. 2, p. 425, Feb. 2018.

[19] M. Liu, W. Pan, and G. Yang, "A new calculation method of short-circuit currents contributed by doubly-fed wind turbines cluster," in *Proc. IEEE 6th Int. Conf. Renew. Energy Res. Appl.*, San Diego, CA, USA, Nov. 2017, pp. 669–673.

[20] *General Administration of Quality Supervision, Inspection and Quarantine of the People's Republic of China, and Standardization Administration of the People's Republic of China, GB/Z 15544 1-2013 Technical Rule for Connecting Wind Farm to Power Network*, Standards Press China, Beijing, China, 2014.

[21] J. Morren and S. W. H. de Haan, "Ridethrough of wind turbines with doubly-fed induction generator during a voltage dip," *IEEE Trans. Energy Convers.*, vol. 20, no. 2, pp. 435–441, Jun. 2005.

[22] J. Lopez, P. Sanchis, X. Roboam, and L. Marroyo, "Dynamic behavior of the doubly fed induction generator during three-phase voltage dips," *IEEE Trans. Energy Convers.*, vol. 22, no. 3, pp. 709–717, Sep. 2007.

[23] M. Gholizadeh, S. Tohidi, A. Oraee, and H. Oraee, "Appropriate crowbar protection for improvement of brushless DFIG LVRT during asymmetrical voltage dips," *Int. J. Elect. Power Energy Syst.*, vol. 95, pp. 1–10, Feb. 2018.

[24] X. Zhang, R. Li, and D. Xu, "Analysis of three-phase short circuit current of DFIG," in *Proc. 13th Eur. Conf. Power Electron. Appl.*, Barcelona, Spain, Sep. 2009, pp. 1–7.

[25] J. Jimmie, *Electric Machines: Analysis and Design Applying MATLAB*. New York, NY, USA: McGraw-Hill, 2001, pp. 264–265.

[26] J. B. Liu and C. H. Zhang, *Electric Machines and Drives*, 2nd ed. Beijing, China: Tsinghua Univ. Press, 2006, pp. 239–240.

[27] S. Yang, T. Zhou, D. Sun, Z. Xie, and X. Zhang, "A SCR crowbar commutated with power converter for DFIG-based wind turbines," *Int. J. Elect. Power Energy Syst.*, vol. 81, pp. 87–103, Oct. 2016.

[28] Y. Gao, Y. Jin, P. Ju, and Q. Zhou, "Dynamic equivalence of wind farm composed of double fed induction generators considering operation characteristic of crowbar," *Power Syst. Technol.*, vol. 39, pp. 628–633, Mar. 2015.
[29] G. Q. Li, *Power System Transient Analysis*, 3rd ed. Beijing, China: China Electric Power Press, 2007, pp. 12–14.
[30] E. Muljadi, S. Pasupulati, A. Ellis, and D. Kosterov, "Method of equivalencing for a large wind power plant with multiple turbine representation," in *Proc. IEEE Power Eng. Soc. Gen. Meeting*, Detroit, MI, USA, Jul. 2009, pp. 1–9.

MINGYANG LIU received the B.S. degree in electrical engineering in 2013. He is currently pursuing the Ph.D. degree in electrical engineering with Hohai University, China. His main research interest focuses on the wind power generation technology.

WENXIA PAN received the B.S. and M.S. degrees from Wuhan University, Wuhan, China, in 1982 and 1987, respectively, and the Ph.D. degree from Hohai University, Nanjing, China, in 2004. She is currently a Professor of electrical engineering with Hohai University, Nanjing. Her current research interests include renewable energy generation system and high voltage and insulation technology. She has authored two research books and authored and co-authored over 100 journal papers.

RUI QUAN received the Ph.D. degree in electrical engineering from Hohai University, Nanjing, China, in 2018. His main research interest focuses on renewable energy generation technology.

HONGYU LI (S'14) received the B.S. degree in electrical engineering in 2012. He is currently pursuing the Ph.D. degree in electrical engineering with Hohai University, Jiangsu, China. He is currently performing research with the University of Tennessee, Knoxville, TN, USA, as a Visiting Student. His main research interest focuses on power system dynamic analysis under stochastic disturbances.

TONGCHUI LIU received the B.S. and M.S. degrees in 2012 and 2015. He is currently pursuing the Ph.D. degree in electrical engineering with Hohai University, Nanjing, China. He is also an Engineer with State Grid Ningbo Power Supply Company, Ningbo, China. His main research interest focuses on renewable energy generation technology.

GANG YANG received the B.S. and M.S. degrees from Hohai University, Nanjing, China, in 2014 and 2017, respectively. He is currently an Assistant Engineer with the Maintenance Branch, Jiangsu Electric Power Company, Xuzhou, China. His main research interest focuses on the wind power generation technology.